The Effect of Electric Field on the Frontier Orbitals of Organic Small Molecules: DFT Studies of Triphenylamine Derivatives

Benjamin Parks and Lichang Wang*
School of Chemical and Biomolecular Sciences, Southern Illinois University, Carbondale, IL 62901, USA

Abstract

The effect of strong electric fields on four triphenylamine derivatives was investigated. Using the optimized structures performed via B3LYP/6-31+G(d,p) level of theory in vacuo, single-point energy calculations were performed in this work with CAM-B3LYP/6-311+G(d,p) with electric fields of strength $50x10^{-4}$au (c.a $2.57x10^{9}$V/m) parallel and antiparallel to each of the x, y, and z axes. While fields in the y- and z- directions had little effect on molecular orbital (MO) contours, large changes occurred for fields in the x-direction, where the molecule lies. Additional calculations were performed at intermediate x-direction field strengths. The changes of the orbital contours are attributed both the pull of the field on the electrons in an orbital and to the rearrangement of molecular orbitals' energies relative to one another. Furthermore, a linear relationship between MO energy and electric field strength was discovered, with deviations from linearity at high field strengths due to the near free electron characteristics. The maximum difference in HOMO and LUMO energy for the molecules under a more realistic field strength of $0.4x10^{-4}$au was estimated to be about 0.022eV, which is insignificant to affect the open voltage of a solar cell device.

*Corresponding author: lwang@chem.siu.edu

1. Introduction

Great progress has been made over the past thirty years in the development of solar cells using organic small molecules, particularly in the form of dye sensitized solar cells (DSSCs)[1-15] and organic solar cells (OSCs).[16-39] Recently, OSCs with an efficiency of 20.8% were achieved.[16] Much work has been done to find suitable dye and donor molecules for DSSCs and ORCs. There are many requirements which must be met for any potential dye or donor molecules, including high thermal and electrical stability, high absorptivity of visible light, anchoring groups (for DSSCs), and appropriate energy of HOMO and LUMO for the system in consideration. However, there are additional requirements and desirable characteristics too. For example, high charge mobility would increase device efficiency by facilitating charge transfer throughout the device, and increasing the stability of the dye/donor molecule's excited state would result in more efficient exciton separation rates.

There are, of course, a practically infinite number of dye/donor molecule candidates. One of the most effective frameworks for computationally rational design of sensitizers is to focus on one set of molecules with similar chemical properties and composition – carefully calibrating the abilities of a particular computational method against experimental results – and then apply the same computational model to similar molecules to predict their properties. Hence, it is desirable to choose a single class of molecules with similar chemical properties and study them, and ideally a class with multiple use cases. Triphenylamine (TPA), as the name implies, is a nitrogen atom bonded with three phenyl rings, and its derivatives have gained a prominent stance in both DSSC and OSC research endeavors for a variety of reasons. Namely, they are known to have a high electron donating ability (as DSSC dyes), a high hole mobility (for dye or donor use), and a high molar absorptivity. Additionally, triphenylamine derivatives have received extensive usage as a

hole transport material (HTM). Hole transport materials fill the role of an electrolyte for a DSSC, but are comprised of a purely solid material, and have the benefit of having simpler dye regeneration mechanisms and being less damaging to the cell than electrolyte solutions. In fact, the TPA derivative Sprio-OMe-TAD [2,2′,7,7′-tetrakis(N,N′-di-p methoxyphenylamine)-9,9′-spirobifluorene] is one of the premier HTM candidates available, being described as a "champion" of the area. The three phenyl rings in TPA are tilted with respect to N-bonding plane, giving a propeller-like molecule shape. This shape gives additional steric hindrance to TPA-based dyes, which could help to prevent electrolyte-anode charge recombination in DSSC setups. Due to these exciting properties, our research group has done extensive work with TPA derivatives over the past 15 years.

One direction of research is investigating derivatives of 4-vinyl-N,N-di(p-tolyl)aniline, abbreviated MTPA, as shown in Figure 1 for a visual representation of the MTPA structure (R=H). This research into the MTPA derivatives began with a similar molecule (MTPA with no methyl groups) which indicated that the 6-31+G(d,p) (and higher levels of theory) provide a reasonable level of accuracy. Shortly thereafter, MTPA modified with additional π-linker and acceptor units was shown to perform well as the dye in a DSSC. Based on the reasonable applicability of MTPA in DSSCs, calculations were performed on several derivatives with different functional groups at the labelled R position of Figure 1. This study investigated the relative merits of H, NH_2, OCH_3, Cl, CN, NO_2, and 2-carboxy-2-cyanovinyl acid functional groups, finding that the 2-caboxy-2-cyanovinyl group gives stellar improvement to electron-hole separation, binding energy, and provides a bidentate anchoring group. Further research with these derivatives confirmed the use of 6-31+G(d,p) basis (or higher) and B3LYP as a relatively accurate functional. Lastly, increasing the charge-separation lifetime of the exciton was investigated by incorporating a D-A_1-A_2 structure[40-

[42] – along with changing the composition of bridging atoms – resulting in specific molecules for further study. In addition to the D-A_1-A_2 architecture, we also studied excitons at single molecule level,[43] the character of charge separated state,[4, 44-47] and the effect of triplet state on the relaxation of electron excitation.[48] We note that many other researchers have also conducted studies of various properties of molecules[49-69] and their functionalization.[70-75] As the organic small molecules (OSMs) are also widely used for sensors,[76-80] especially organic long-persistent luminescence sensors,[81, 82] their synthesis[83] has been an active area of research.

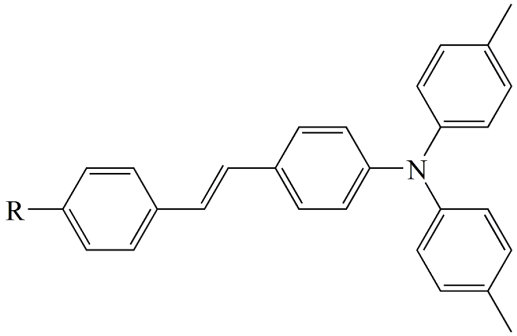

Figure 1. Structure of MTPA derivatives.

In solar cell devices, OSMs as sensitizers are aggregates. These aggregates often have different properties than those of single molecules. The effect of aggregate on the device performance has attracted a lot of research efforts.[84-92] In particular, polar materials possess a built-in electric field and can also be effective for catalysis.[93-112], which is one of the reasons on why alloys have unique properties[113] or tuning oxidation state of catalysts[114] and may be explored for better catalysis for ethanol oxidation reaction[115-119] or steam reform of hydrocarbons.[120] A review of the electric field on various properties can be found.[121, 122] The effect of electric field has been used in the design of biomolecules[123, 124] and decomposing Alzheimer's.[125] Because of the importance of electric field, there were extensive efforts to develop measurements of these electric fields.[126-144]

Computationally, there were DFT studies of E-field.[145-147] and Machine-learning prediction.[148] Studies can also be found on the charge density site on catalysts[149-151] and molecules.[8, 152-161] Studies of sensing under electric field were also conducted.[162, 163]

The effect of an electric field on dye/donor molecules has been investigated in literature,[8, 60, 147, 161, 164, 165] but there is a lack of investigation into these effects on triphenylamine derivatives. In this work, calculations were performed on four MTPA derivatives. They are shown in Figure 2. The ordering of MTPABT-Pyc, MTPAcc, MTPAcc-Pyc, MTPACo-Pyc will be maintained, as it corresponds to the ordering of the molecules' dipole moments from greatest to least.

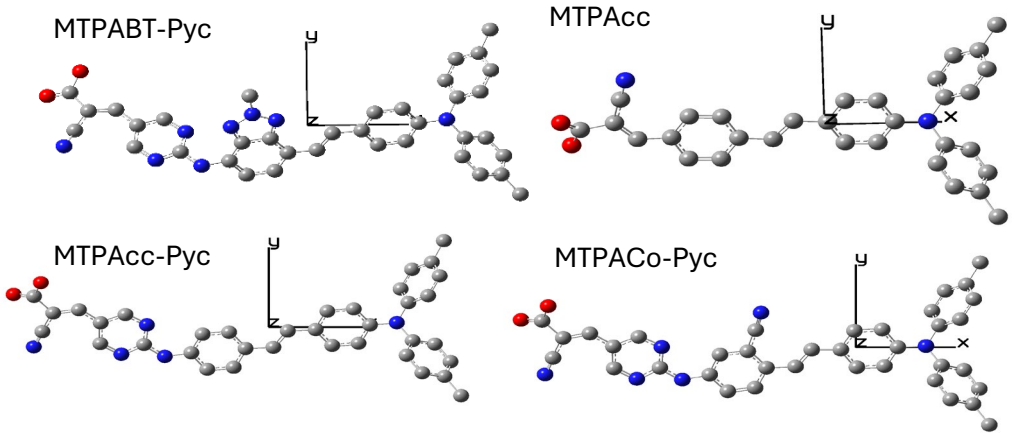

Figure 2. Structures for MTPABT-Pyc, MTPAcc, MTPAcc-Pyc, and MPTACo-Pyc. H atoms are removed for clarity.

2. Computational Details

The computational software used in this work is Gaussian16W with the GaussView6.0 user-interface. For each molecule, an optimization calculation was performed previously,[70] using B3LYP functional,[166, 167] and a 6-31+G(d,p) basis set in vacuo. These molecules are aligned such that the length of the molecule is parallel to the x-axis and the planar conjugated regions lie in the x-y plane. Using the optimized structures, single-point energy calculations were performed in this work on each molecule with an applied electric field in the positive and negative x, y, and z-

directions. A default convergency criterion for electronic optimization at a sing-point was used, just as in our previous DFT studies.[168] The fixed orientation is to mimic the aggregates where single molecules are confined. The DFT results at a single-point geometry will represent the upper limit of changes in the properties compared to the results where the molecules are allowed to relax in respond to the external field.

These single-point energy calculations were performed using the CAM-B3LYP functional[169] and 6-311+G(d,p) basis set with symmetry ignored. Initially, the field strengths ranged from -50x10^{-4}au to +50x10^{-4}au. The standard electric field value in atomic units is 1au≈5.142x10^{11} V/m, so 50x10^{-4}au≈2.57x10^{9} V/m. This value should be compared to the internal field strength for solar cells (c.a. 0.4x10^{-4} au=2.1x10^{7}V/m) which is randomly oriented in OSC devices and has average direction between the electrodes of DSSC devices.[147,165] Clearly, this range is far wider than what experimental conditions are expected to vary as; however, other studies have considered field strengths up to 25x10^{-4}au, validating the scope of this study.[147, 161]

3. Results

DFT results on the molecular orbital contours and energies at the electric field of 50x10^{-4}au are shown in Figures 3-6. We note that the electric field was applied in various directions. Figures 3-6 showcase the effect of the strongest field strength on the four frontier orbitals of each molecule (HOMO-1 through LUMO+1) via molecular orbital visualizations. The visualization with no field is shown at the top of each page for comparison. These electric fields have a magnitude of 50x10^{-4}au with direction parallel or antiparallel to the x, y, and z axes. This is represented through the standard $< \hat{\imath}, \hat{\jmath}, \hat{k} >$ vector notation.

Figure 3 shows the MO visualizations for the MTPABT-Pyc molecule. For the molecule with no applied field, the HOMO and HOMO-1 orbitals are located primarily on the donor-moiety, with

some additional density throughout the π-linker. Conversely, the LUMO orbital is primarily centered on the acceptor moiety, and the LUMO+1 orbital on the π-linker. When a field is applied in the positive x-direction, electrons are pulled opposite to the field (due to their negative charge) and thus shift toward the acceptor moiety, increasing the magnitude of charge separation. This is corroborated by a significantly higher dipole moment of $\overrightarrow{\mu_x} = 21.5D$ for this molecule compared to the 0-field value of $\overrightarrow{\mu_x} = 11.5D$. Conversely, an electric field in the negative x-direction pulls the electrons toward the donor-moiety. In fact, $\overrightarrow{\mu_x} = -1.4D$, suggesting that the phenyl rings command more of the electronic charge than the cyano- and carboxylic acid groups. Note that, in a DSSC setup, these two cases would represent the electric field pointing out from and into the TiO_2 surface, respectively. Furthermore, both cases have drastically shifted molecular orbitals. This is especially pronounced for the (-) x-direction field, wherein every orbital is centered on a totally different moiety than for the 0-field molecule. For the fields applied along the y- and z-axes, much less difference is noticeable. Specifically, the basic shapes of each of the MOs shown are the same for all four of these calculations. There are some slight differences – for example, the donor phenyl rings of the HOMO-1 orbital along the (+) and (-) y-direction – but these differences are much less significant than for the x-direction.

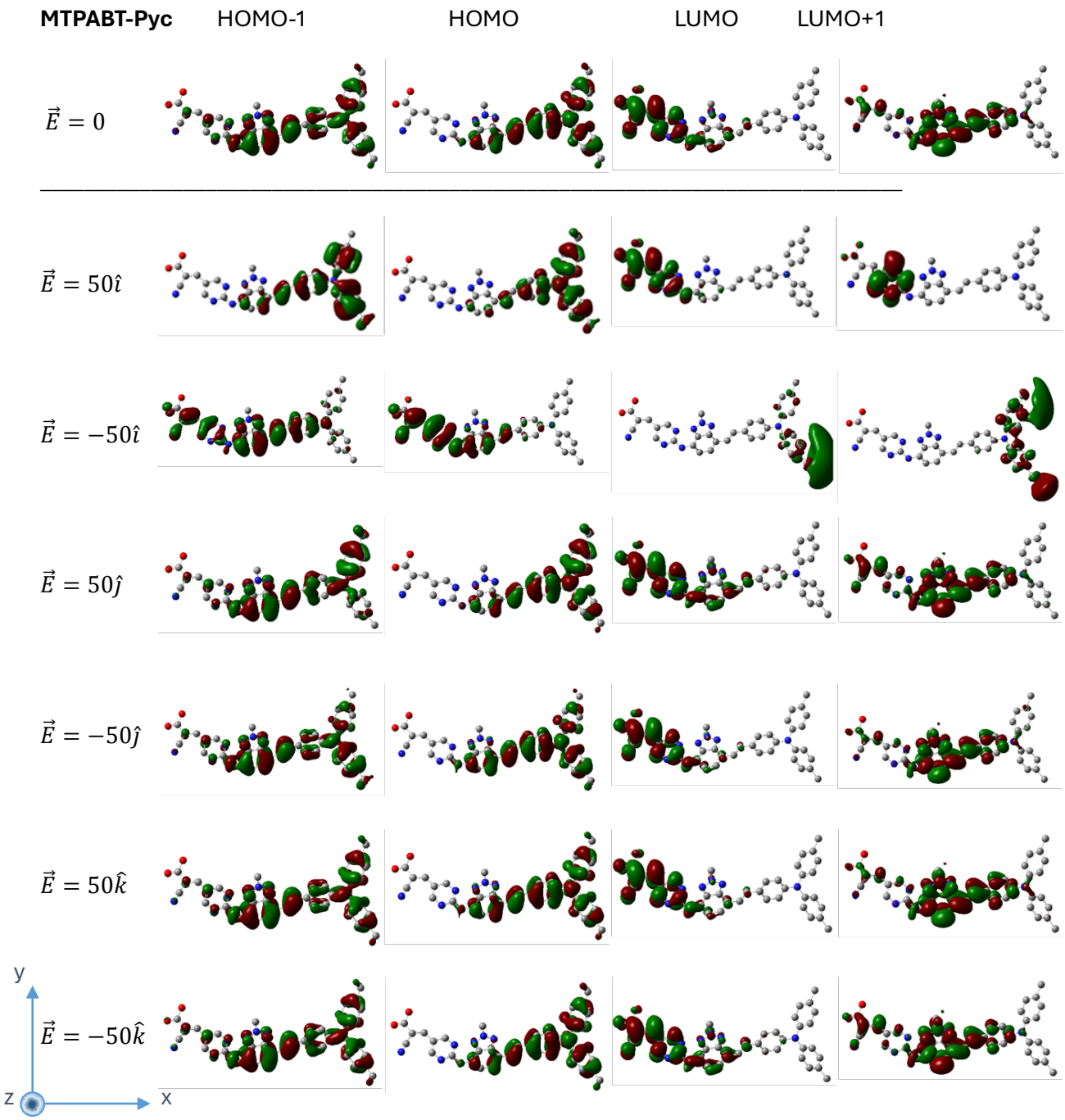

Figure 3. Molecular Orbital Visualizations for MTPABT-Pyc. H atoms are removed for clarity. The values shown are in 10^{-4}au field strength. Cartesian axes are shown for reference.

For the remaining molecules, shown in Figures 4-6, very similar explanations are appropriate. Having a field pointing along or against the x-direction produces enormous differences, with an

entire rearrangement of the relative energies of the molecular orbitals. Additionally, any fields in the y- and z-directions produce much smaller effects, with only minor reconfigurations of the position of the electrons. Again, the phenyl rings of the LUMO+1 visualizations showcase these minor differences well under (+) and (-) y-direction fields.

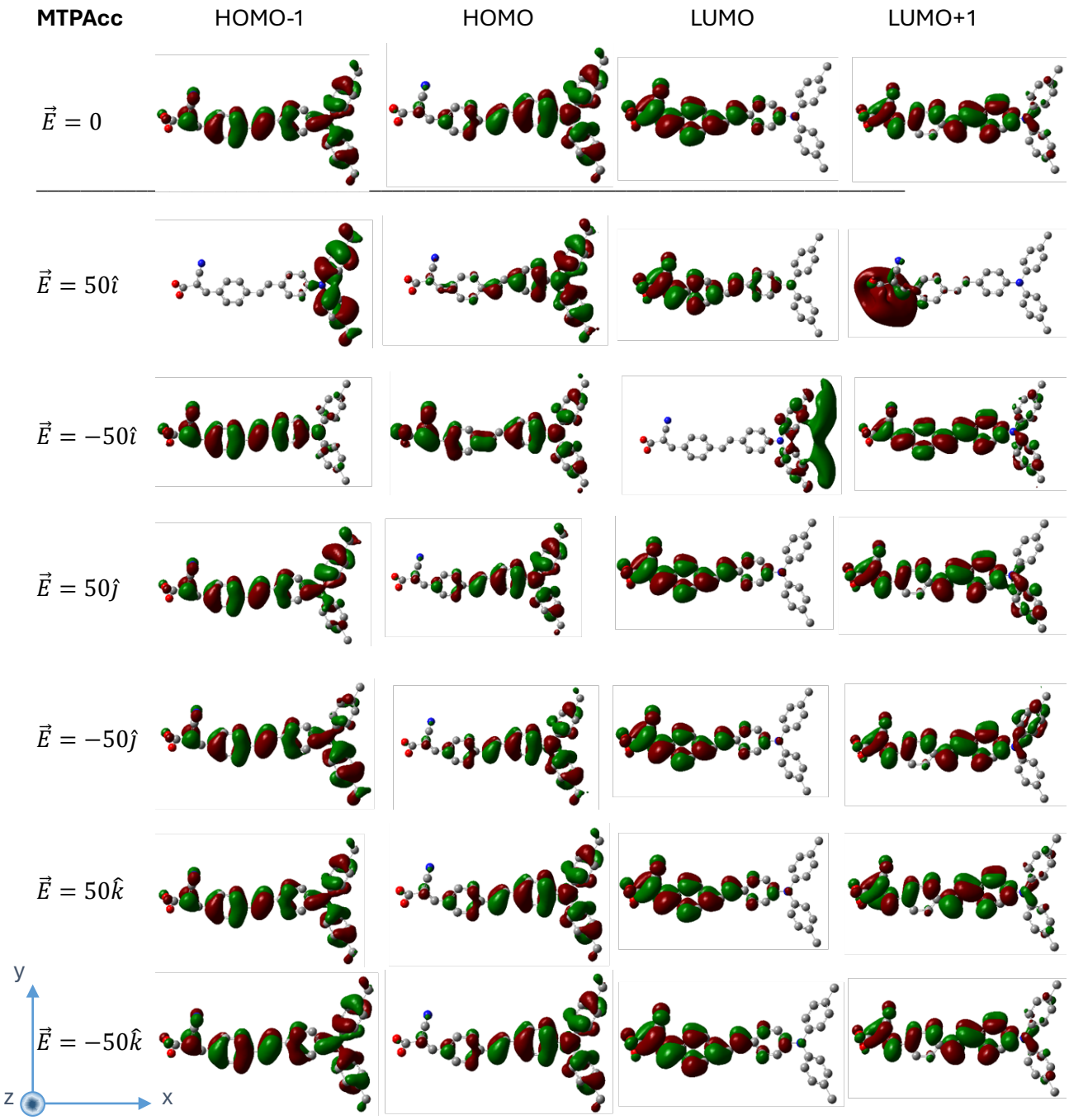

Figure 4. Molecular orbital visualizations for MTPAcc. H atoms are removed for clarity. The values shown are in 10^{-4}au field strength. Cartesian axes are shown for reference.

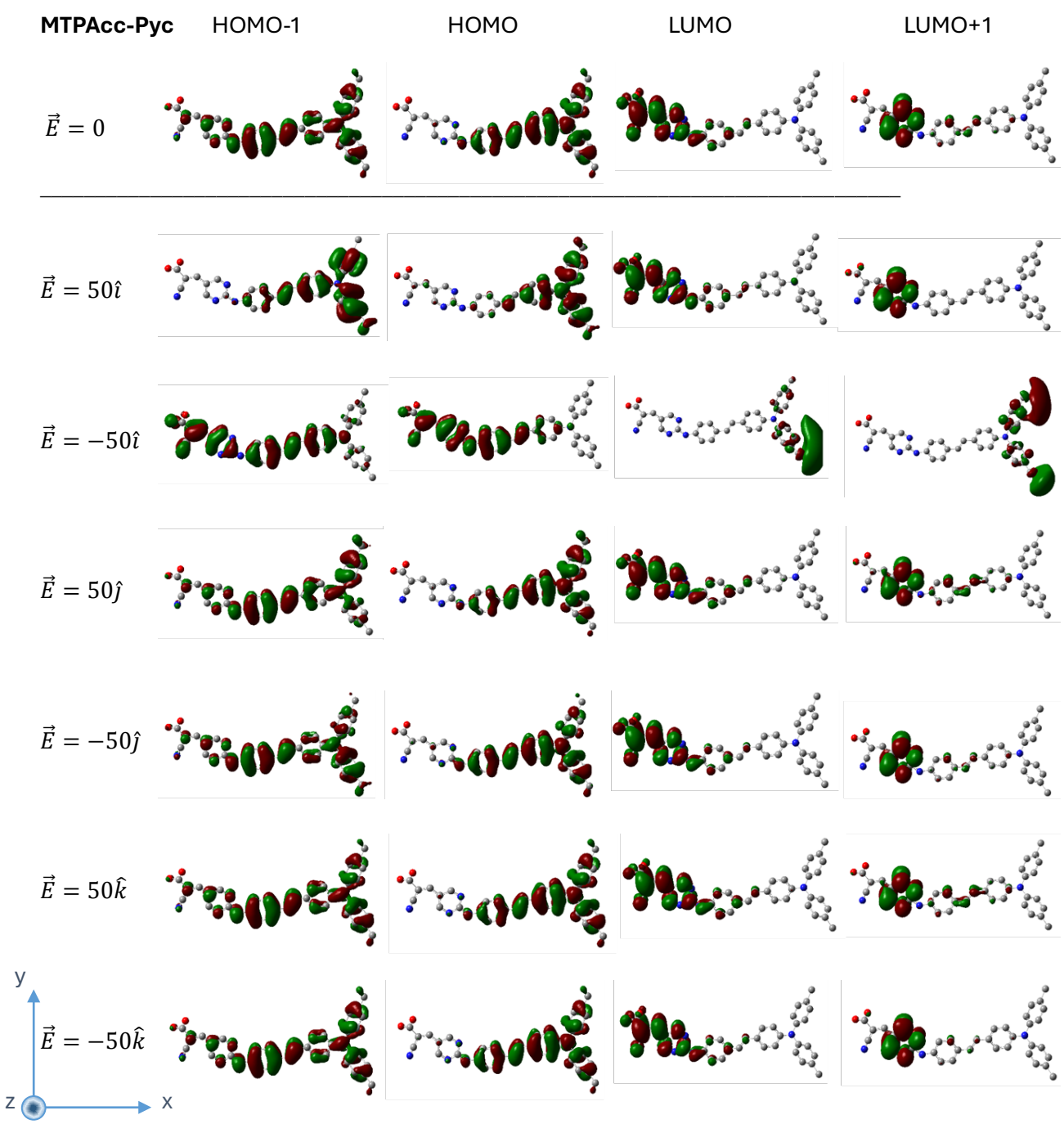

Figure 5. Molecular orbital visualizations for MTPAcc-Pyc. H atoms are removed for clarity. The values shown are in 10^{-4}au field strength. Cartesian axes are shown for reference.

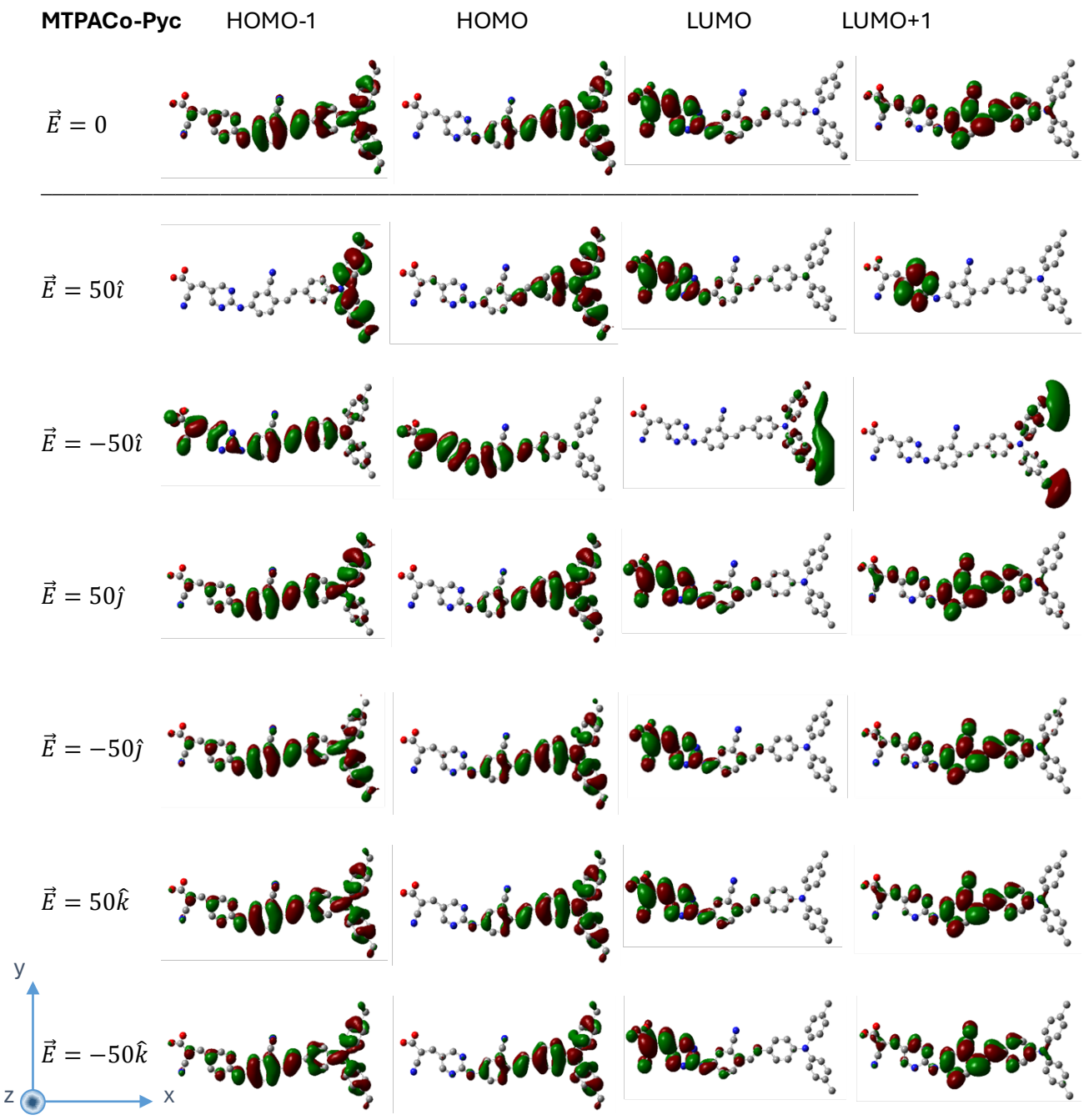

Figure 6. Molecular orbital visualizations for MTPACo-Py. H atoms are removed for clarity. The values shown are in 10^{-4}au field strength. Cartesian axes are shown for reference.

In addition to the y- and z-direction fields having small visual effect, there is only a minute energetic effect. The energies of the HOMO and LUMO of MTPABT-Pyc under various y- and z-field strengths are given in Table 1 to showcase this. It is noted that MTPABT-PYC experienced the greatest variation of the four molecules. With a maximum energy difference of 0.2eV under field strengths c.a. 100X greater than experimental conditions, we conclude that there is not expected to be a significant difference for y- and z-fields.[165]

Table1. MO Energies for MTPABT-Pyc versus y- and z-fields.

Field Strength (10^{-4} au)	$50\hat{\imath}$	$40\hat{\imath}$	$20\hat{\imath}$	$0\hat{\imath}$	$-20\hat{\imath}$	$-40\hat{\imath}$	$-50\hat{\imath}$	$50\hat{k}$	$30\hat{k}$	$0\hat{k}$	$-30\hat{k}$	$-50\hat{k}$
HOMO (eV)	-6.32	-6.29	-6.31	-6.33	-6.31	-6.30	-6.29	-6.34	-6.39	-6.33	-6.32	-6.31
LUMO (eV)	-1.90	-1.87	-1.89	-1.92	-1.94	-1.96	-1.97	-2.01	-2.03	-1.92	-1.88	-1.86

With the drastic changes noted for fields applied along the x-direction, investigation into the effects of more intermediate fields is in order, especially to see the effects fields of strength more approximating experimental conditions. Figures 7-10 show the effect of a changing field strength in only the x-direction. Again, the HOMO-1 through LUMO+1 molecular orbital visualizations are included, with the field strengths including 0, $\pm 10 \times 10^{-4}$, $\pm 20 \times 10^{-4}$, and $\pm 35 \cdot 10^{-4}$au. Note that the 0-field visualizations are shown in the middle of the Figure, as opposed to the top of the page in Figures 3-6.

The expected trends are observed in these visualizations. Namely, fields in the positive direction tend to draw the electrons towards the acceptor moiety and fields in the negative direction tend to draw electrons towards the donor moiety, with these effects being more pronounced with increasing field strength. We speculate that these visual differences are caused by two main factors. Firstly, the electrons within an orbital will shift slightly, either opposite to the field due to its

effects, or along the field due to the attraction of nuclei that have become deprived of electron density. The MTPAcc-Pyc LUMO showcases this movement well between $+35\hat{\imath}$ and $-20\hat{\imath}$. Additionally, the relative ordering of orbital energies will change. In other words, the field may increase the energy of one orbital and decrease the energy of another, causing them to "swap." The MTPAcc-Pyc LUMO+1 orbital showcases this well, with the field strengths of $+35\hat{\imath}$ through 0 having orbital contours distinct from those of $-10\hat{\imath}$ and $-20\hat{\imath}$, which are further distinct from -$-35\hat{\imath}$.

While all four molecules have noticeable differences in their MO visualizations between the $10\hat{\imath}$ and $-10\hat{\imath}$ field strengths, only the MTPAcc-Pyc molecule has two MOs swap in energy as described. Again, $10\hat{\imath}$ corresponds to a field strength of $10\text{x}10^{-4}$au, which is c.a. 20X stronger than would be expected in a typical solar cell.[165] Hence, it is unlikely that such an effect would be encountered there. This is an encouraging result, as orbital rearrangement could result in reduced efficiency by excited electrons not being properly sent from the donor to the acceptor moiety.[43]

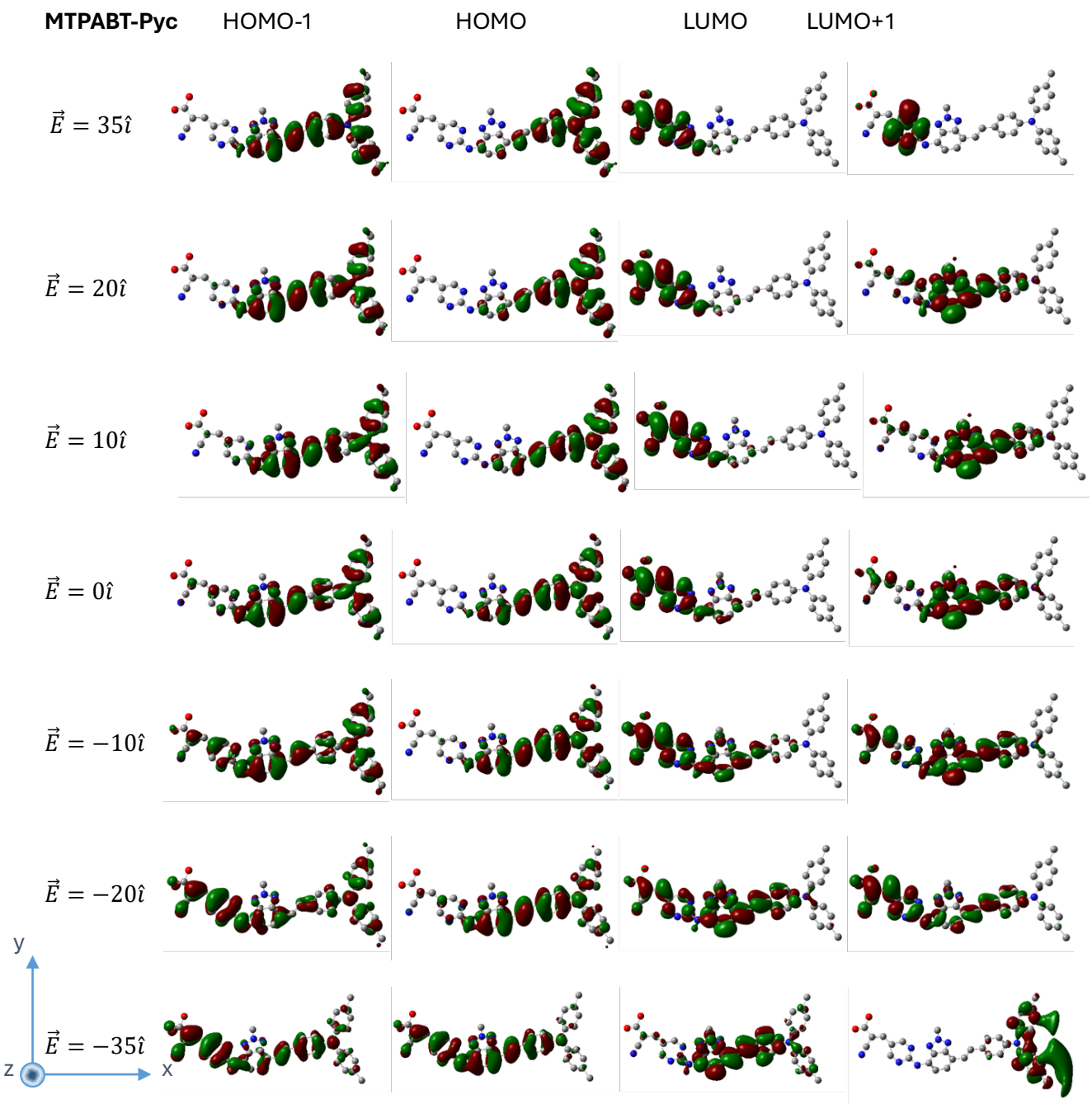

Figure 7. MTPABT-Pyc: Molecular orbital visualizations with varying x-field strengths. H atoms are removed for clarity. The values shown are in 10^{-4}au field strength. Cartesian axes are shown for reference.

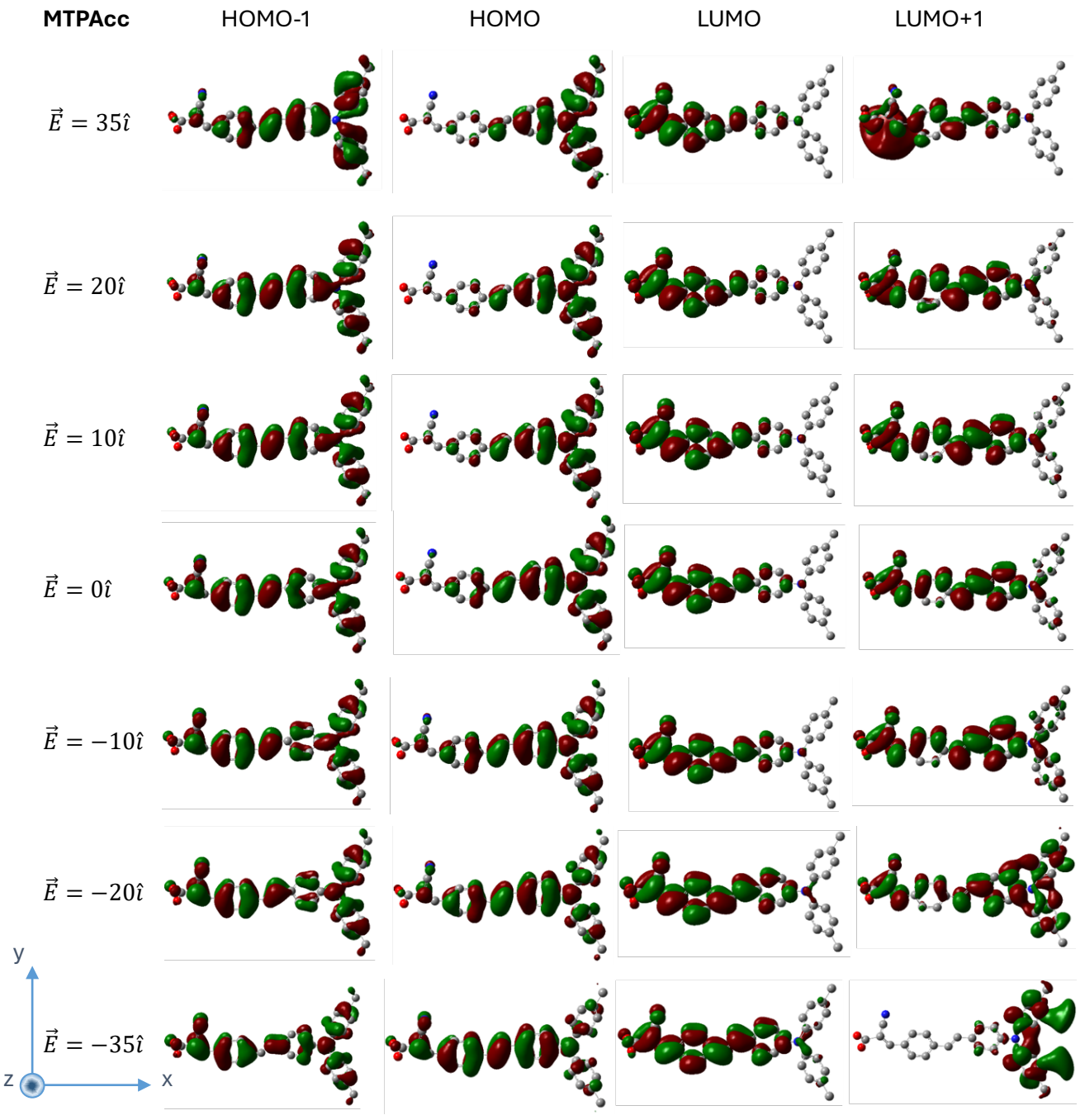

Figure 8. MTPAcc: Molecular orbital visualizations with varying x-field strengths. H atoms are removed for clarity. The values shown are in 10^{-4}au field strength. Cartesian axes are shown for reference.

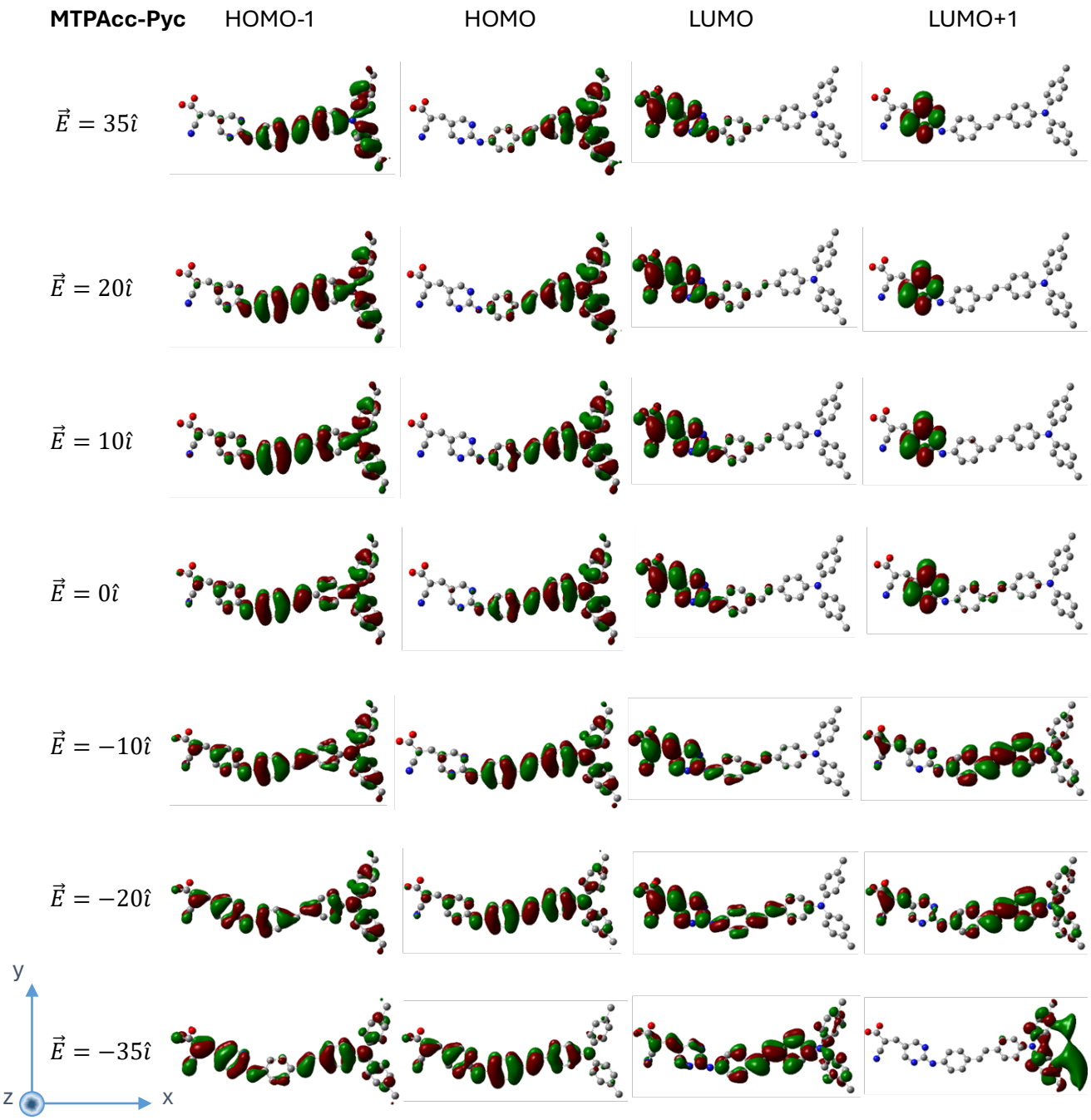

Figure 9. MTPAcc-Pyc: Molecular orbital visualizations with varying x-field strengths. H atoms are removed for clarity. The values shown are in 10^{-4}au field strength. Cartesian axes are shown for reference.

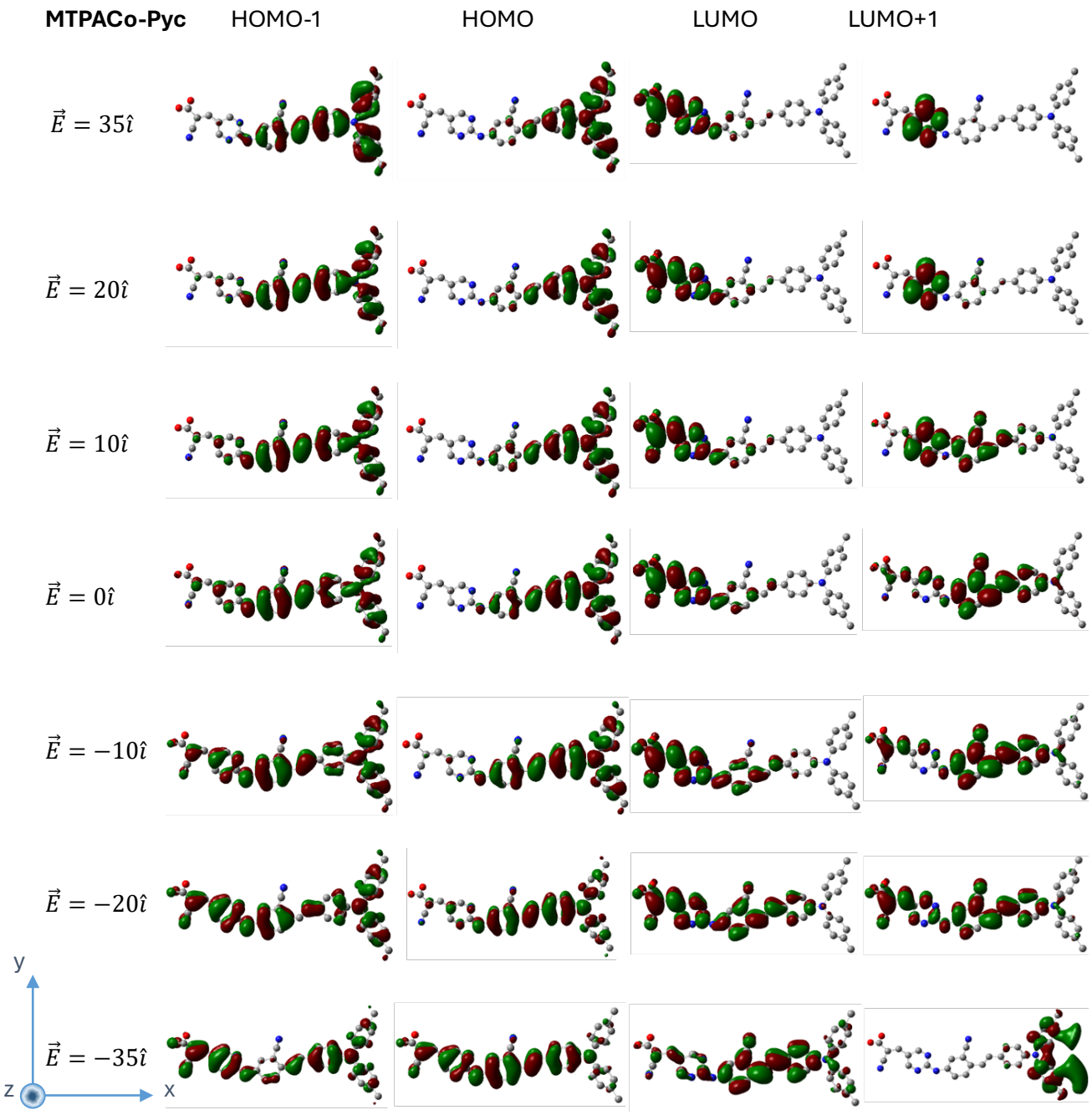

Figure 10. MTPACo-Pyc: Molecular orbital visualizations with varying x-field strengths. H atoms are removed for clarity. The values shown are in 10^{-4}au field strength. Cartesian axes are shown for reference.

Again, the MO shapes are not the only factor to consider – the orbitals are also changing in energy. Due to the stringent requirements of HOMO and LUMO energies for both OSC and DSSC

devices, this could be an enormous issue. As such, Figure 11 shows the energies of the frontier orbitals for each molecule as the magnitude of x-direction field is altered.

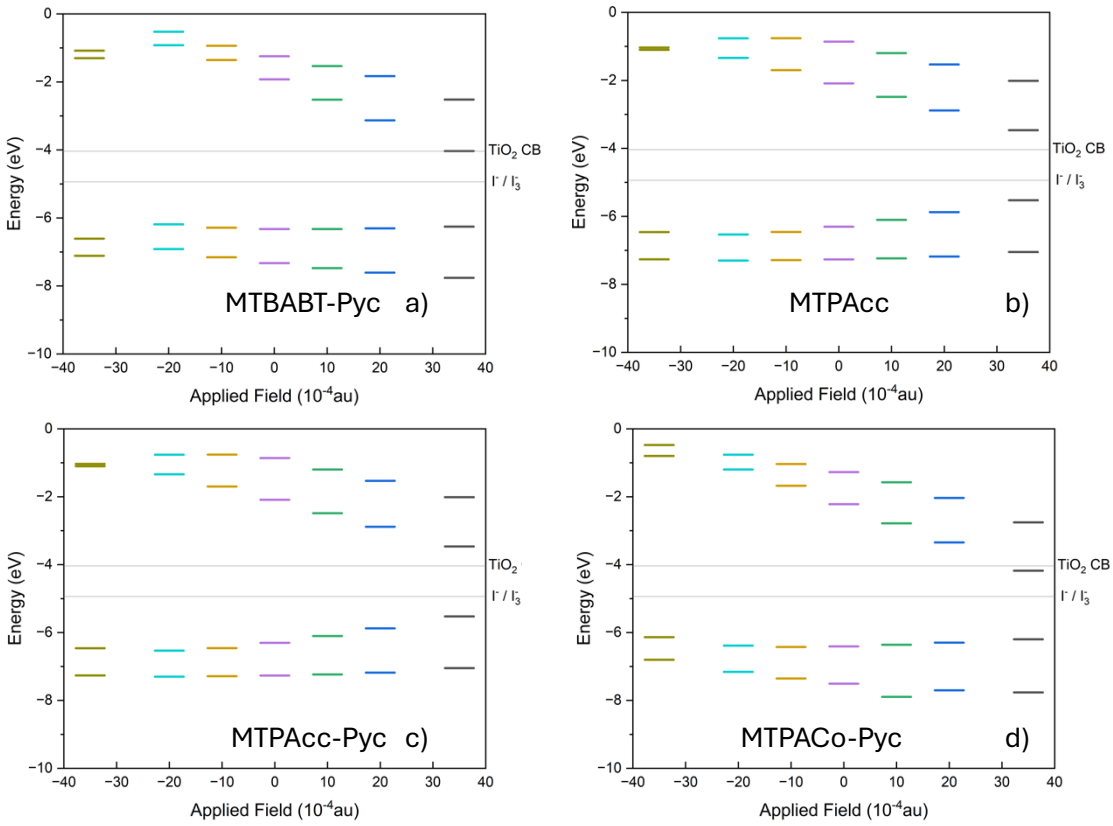

Figure 11. Frontier orbital energies at various applied fields along the X-axis. The HOMO-1 through LUMO+1 orbitals are included for MTPABT-Pyc in a), MTPAcc in b), MTPAcc-Pyc in c), and MTPACo-Pyc in d)

As can be seen in Figure 11, the basic trend is similar for each molecule. The LUMO and LUMO+1 energies increase for fields in the (-) x-direction and decrease for fields in the (+) x-direction. The HOMO and HOMO-1 energies appear to have the opposite trend but are not as strongly affected. In fact, the significantly larger effect experienced by the virtual MOs suggests that these differences are likely over estimated. It is suggested that calculating the LUMO energy via the anionic species could give more accurate results, as has been shown in our other works,[170] though experimental verification of this could be difficult.

Interestingly, the above graphs suggest a locally linear trend between an orbital energy and the applied field strength. This is not unexpected, as the potential energy of a fixed dipole in an electric field is equal to the dot product of the dipole moment and field strength.[171] This linear trend is particularly evident for the LUMO and LUMO+1 orbitals and the MTPAcc and MTPAcc-Pyc HOMO orbitals, while the lack of change for the MTPABT-Pyc and MTPACo-Pyc HOMOs makes trends hard to discern. Furthermore, this appears to become less true as the field strength increases, which is attributed to rearrangement of the electrons to a lower-energy state (i.e., this dipole is not fixed). To investigate this, the HOMO and LUMO energies for each molecule are plotted versus field strength in Figure 12, with the origin fixed at the 0-field MO energies. The $35x10^{-4}$au fields are omitted due to significant rearrangements.

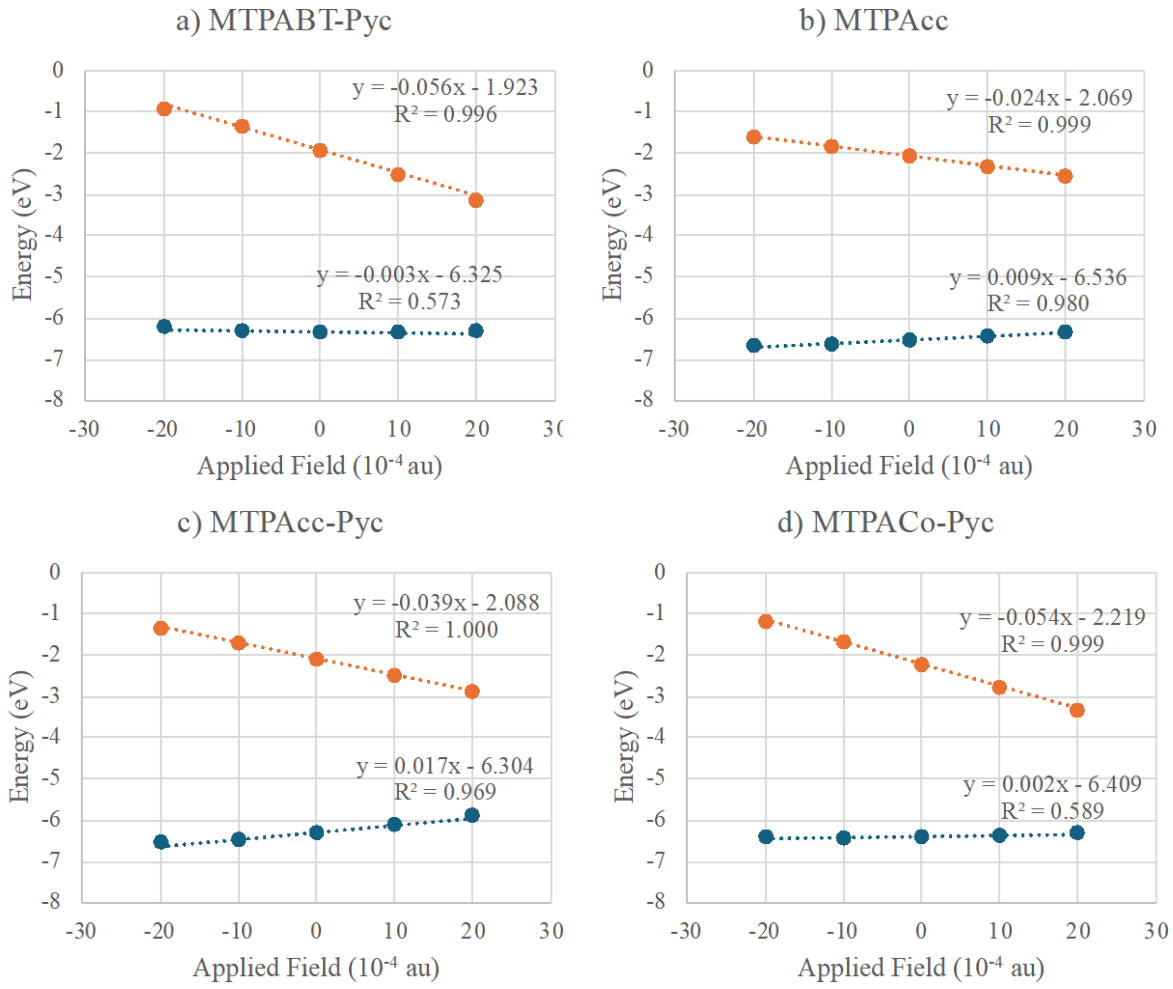

Figure 12. The HOMO & LUMO energies as a function of applied field.

Excluding the afore-mentioned HOMO trends, the linear approximations fit quite well. Furthermore, the literature value electric field strength of 0.4×10^{-4}au,[165] combined with the maximum slope value obtained above ($0.056 \text{eV}/10^{-4}$au for the MTPABT-Pyc LUMO) gives an error prediction of 0.022eV. Clearly this value is too small to impact the functionality of the solar cell from an energetics standpoint. It is further noted that the opposite slope signs for the HOMO and LUMO energies indicate that errors for the HOMO and LUMO are cumulative towards calculating the HOMO-LUMO gap, though the predicted error would still be minute. Hence, it is

unlikely that electric fields are a large factor for MTPA-type molecules in DSSCs/OSCs. However, the orientation of molecules in aggregates can be influenced by the external electric field and may offer an effect tool to orientate molecules in desirable ways.

4. Conclusions

MTPA-derivatives were studied with their structures taken from our previous works using B3LYP/6-31+ G(d,p) method. Using these optimized structures, we performed single-point energy calculations using CAM-B3LYP and 6-311+ G(d,p) basis set with applied electric fields. These electric fields had magnitudes of $50x10^{-4}$au, or approximately $2.57x10^{9}$V/m. From these calculations, the effects of the electric fields in various directions were investigated on the molecular orbital contours. While fields in the y- and z- directions had little effect, fields applied in the x-direction had large effects, so additional calculations were performed at intermediate field strengths in the x-direction. The changes of the orbital contours are attributed to slight differences of specific orbitals caused by the pull of the field on the electron, and to the rearrangement of the energies of the molecular orbitals relative to one another. Furthermore, the energies of any particular molecular orbital in an electric field follow an approximately linear trend, explained by treating the orbital as dipole, with deviations at high field strengths due to the rearrangement of the electron density. This linear trend was used to predict the maximum difference in HOMO and LUMO energy for the molecules under a realistic solar cell field strength of $0.4x10^{-4}$au, with the resulting errors being relatively small. The errors of the HOMO and LUMO predictions are expected to be cumulative (and not cancel), but still have small enough magnitude to not be of concern. Further studies should be undertaken at weaker field strengths (i.e. $1–5x10^{-4}$au) to confirm the linear approximation used. These data suggest that electric fields are not a significant factor for dye/donor usage of the studied MTPA derivatives; however, it remains unclear how similar

field strengths would impact the functionality of other molecules. Furthermore, this study excluded the TiO_2 substrate, which could have a massive impact on the electric properties of the molecules for DSSC use. Specifically, the TiO_2 substrate would be located along the x-axis used here, which could have a significant impact on which MOs have the frontier energies, and thus greatly impact charge separation and electron injection.

Acknowledgements

We thank Dr. Thomas Testoff for providing the geometry data of the molecules studied in this work and his help during DFT calculations. Ben Parks acknowledges the financial support from the REACH program of the Southern Illinois University Carbondale and the Illinois Soybean Center.

References

1. X. Wang, B. Zhao, W. Kan, Y. Xie and K. Pan, *Adv. Mater.*, 2022, **9**, 2101229.
2. S. Venkatesan, T.-H. Hsua, X.-W. Wong, H. Teng and Y.-L. Lee, *Chem. Eng. J.*, 2022, **446**, 137349.
3. D. Koteshwar, S. Prasanthkumar, S. P. Singh, T. H. Chowdhury, I. Bedja, A. Islam and L. Giribabu, *Mater. Chem. Front.*, 2022, **6**, 580-592.
4. F. Ge, F. Xu, K. Gong, D. Liu, W. Li, L. Wang and X. Zhou, *Dyes Pigm.*, 2022, **200**, 110127.
5. A. B. Munoz-Garcia, I. Benesperi, G. Boschloo, J. J. Concepcion, J. H. Delcamp, E. A. Gibson, G. J. Meyer, M. Pavone, H. Pettersson, A. Hagfeldt and M. Freitag, *Chem. Soc. Rev.*, 2021, **50**, 12450-12550.
6. M. Kokkonen, P. Talebi, J. Zhou, S. Asgari, S. A. Soomro, F. Elsehrawy, J. Halme, S. Ahmad, A. Hagfeldt and S. G. Hashmi, *J. Mater. Chem. A*, 2021, **9**, 10527-10545.
7. G. R. Kandregula, S. Mandal, C. Mirle and K. Ramanujam, *J. Photochem. Photobiol. A: Chem.*, 2021, **419**, 113447.
8. Y. Gao, W. Guan, L.-K. Yan, R. Jia and Z.-M. Su, *Materials Chemistry Frontiers*, 2021, **5**, 929-936.
9. L. Fagiolari, E. Varaia, N. Mariotti, M. Bonomo, C. Barolo and F. Bella, *Adv. Sust. Systems*, 2021, **5**, 2100025.
10. MatteoBonomo, A. Carella, F. Borbone, L. Rosato, D. Dini and L. Gontrani, *Dye Pigm.*, 2020, **175**, 108140.
11. N. Mariotti, M. Bonomo, L. Fagiolari, N. Barbero, C. Gerbaldi, F. Bella and C. Barolo, *Green Chem.*, 2020, **22**, 7168-7218.
12. Q. Huaulmé, V. M. Mwalukuku, D. Joly, J. Liotier, Y. Kervella, P. Maldivi, S. Narbey, F. Oswald, A. J. Riquelme, J. A. Anta and R. Demadrille, *Nat. Energy*, 2020, **5**, 468-477.
13. B. Xu, L. Tian, A. S. Etman, J. Sun and H. Tian, *Nano Energy*, 2019, **55**, 59-64.
14. J. Gong, K. Sumathy, Q. Qiao and Z. Zhou, *Renew. Sust. Energy Rev.*, 2017, **68**, 234-246.

15. XiaoqiangYu, Z. Ci, T. Liu, X. Feng, C. Wang, T. Ma and MingBao, *Dyes Pigm.*, 2014, **102**, 126.
16. L. Zhu, M. Zhang, G. Zhou, Z. Wang, W. Zhong, J. Zhuang, Z. Zhou, X. Gao, L. Kan, B. Hao, F. Han, R. Zeng, X. Xue, S. Xu, H. Jing, B. Xiao, H. Zhu, Y. Zhang and F. Liu, *Joule*, 2024, **8**, 3153-3168.
17. X. Zhou, W. Liang, R. Ma, C. Zhang, Z. Peng, T. Archie, D. Pena, J. Wu, Z. Ma, Y. Liao, G. Li and H. Hu, *Energy Environ. Sci.*, 2024, **17**, 7762-7771.
18. X. Yang, Y. Gao, L.-Y. Xu, X. Wu, X. Chen, Y. Shao, B. Xiao, S. Liu, J. Xia, R. Sun and J. Min, *Energy Environ. Sci.*, 2024, **17**, 5962-5971.
19. Y. Wei, Y. Cai, X. Gu, G. Yao, Z. Fu, Y. Zhu, J. Yang, J. Dai, J. Zhang, X. Zhang, X. Hao, G. Lu, Z. Tang, Q. Peng, C. Zhang and H. Huang, *Adv. Mater.*, 2024, **36**, 2304225.
20. Y. Wang, K. Sun, C. Li, C. Zhao, C. Gao, L. Zhu, Q. Bai, C. Xie, P. You, J. Lv, X. Sun, H. Hu, Z. Wang, H. Hu, Z. Tang, B. He, M. Qiu, S. Li and G. Zhang, *Adv. Mater.*, 2024, **36**, 2411957.
21. Z. Luo, W. Wei, R. Ma, G. Ran, M. H. Jee, Z. Chen, Y. Li, W. Zhang, H. Y. Woo and C. Yang, *Adv. Mater.*, 2024, **36**, 2407517.
22. K. Liu, Y. Jiang, G. Ran, F. Liu, W. Zhang and X. Zhu, *Joule*, 2024, **8**, 835-851.
23. H. Liu, Y. Geng, Z. Xiao, L. Ding, J. Du, A. Tang and E. Zhou, *Adv. Mater.*, 2024, **36**, 2404660.
24. B. Hu, S. Gao, X. Wang, F. Cao, Y. Chen, J. Zhang, L. Bu, X. Song and G. Lu, *Energy Environ. Sci.*, 2024, **17**, 7803-7815.
25. X. Xu, W. Jing, H. Meng, Y. Guo, L. Yu, R. Li and Q. Peng, *Adv. Mater.*, 2023, **35**, 2208997.
26. E. K. Solak and E. Irmak, *RSC Adv.*, 2023, **13**, 12244-12269.
27. G. Zhang, F. R. Lin, F. Qi, T. Heumüller, A. Distler, H.-J. Egelhaaf, N. Li, P. C. Y. Chow, C. J. Brabec, A. K.-Y. Jen and H.-L. Yip, *Chem. Rev.*, 2022, **122**, 14180-14274.
28. Z. Yin, Q. Wang, H. Zhao, H. Wang, N. Li and W. Song, *Energy & Environmental Materials*, 2022, **6**, e12443.
29. C. Xu, Z. Zhao, K. Yang, L. Niu, X. Ma, Z. Zhou, X. Zhang and F. Zhang, *J. Mater. Chem. A*, 2022, **10**, 6291-6329.
30. Y. Li, W. Huang, D. Zhao, L. Wang, Z. Jiao, Q. Huang, P. Wang, M. Sun and G. Yuan, *Molecules*, 2022, **27**, 1800.
31. B. P. Dash, S. K. Beriha, B. Naik and P. K. Sahoo, *Materials Today: Proceedings*, 2022, **67**, 1057-1063.
32. M.-Y. Ni, S.-F. Leng, H. Liu, Y.-K. Yang, Q.-H. Li, C.-Q. Sheng, X. Lu, F. Liu and J.-H. Wan, *J. Mater. Chem. C*, 2021, **9**, 3826.
33. J.-W. Lee, D. Jeong, D. J. Kim, T. N.-L. Phan, J. S. Park, T.-S. Kim and B. J. Kim, *Energy Environ. Sci.*, 2021, **14**, 4067-4076.
34. Z. Chen, W. Song, K. Yu, J. Ge, J. Zhang, L. Xie, R. Peng and Z. Ge, *Joule*, 2021, **5**, 2395-2407.
35. X. Wan, C. Li, M. Zhang and Y. Chen, *Chem. Soc. Rev.*, 2020, **49**, 2828-2842.
36. L. Nian, Y. Kan, K. Gao, M. Zhang, N. Li, G. Zhou, S. B. Jo, X. Shi, F. Lin, Q. Rong, F. Liu, G. Zhou and A. K.-Y. Jen, *Joule*, 2020, **4**, 2223-2236.
37. L. X. Chen, *ACS Energy Lett.*, 2019, **4**, 2537-2539.
38. S. Li, L. Ye, W. Zhao, S. Zhang, S. Mukherjee, H. Ade and J. Hou, *Adv. Mater.*, 2016, **28**, 9423-9429.

39. W. T. Hadmojo, S. Y. Nam, T. J. Shin, S. C. Yoon, S.-Y. Jang and I. H. Jung, *J. Mater. Chem. A*, 2016, **4**, 12308.
40. T. Wang, K. C. Weerasinghe, D. Liu, W. Li, X. Yan, X. Zhou and L. Wang, *J. Mater. Chem. C*, 2014, **2**, 5466.
41. T. Wang, H. Sun, L. Zhang, N. D. Colley, C. N. Bridgmohan, D. Liu, W. Hu, W. Li, X. Zhou and L. Wang, *Dyes Pigm.*, 2017, **139**, 601.
42. H. Sun, P. Li, D. Liu, T. Wang, W. Li, W. Hu, L. Wang and X. Zhou, *J. Photochem. Photobiol. A: Chem.*, 2019, **368**, 233-241.
43. T. Wang, K. C. Weerasinghe, P. C. Ubaldo, D. Liu, W. Li, X. Zhou and L. Wang, *Chem. Phys. Lett.*, 2015, **618**, 142-146.
44. H. Sun, D. Liu, T. Wang, T. Lu, W. Li, S. Ren, W. Hu, L. Wang and X. Zhou, *ACS Appl. Mater. Interfaces*, 2017, **9**, 9880-9891.
45. H. Sun, D. Liu, T. Wang, P. Li, C. N. Bridgmohan, W. Li, T. Lu, W. Hu, L. Wang and X. Zhou, *Org. Electronics*, 2018, **61**, 35-45.
46. T. Wang, M. Liu, W. Feng, R. Cao, Y. Sun, L. Wang, D. Liu, Y. Wang, T. Wang and W. Hu, *Adv. Opt. Mater.*, 2023, **11**, 2202613.
47. W. Feng, P. a. Li, H. Sun, D. Liu, L. Wang, X. Zhou, W. Li and T. Wang, *J. Mol. Struct.*, 2019, **1196**, 604-610.
48. T. Wang, K. C. Weerasinghe, H. Sun, X. Hu, T. Lu, D. Liu, W. Hu, W. Li, X. Zhou and L. Wang, *J. Phys. Chem. C*, 2016, **120**, 11338-11349.
49. X. Zhou, D. Liu, T. Wang, X. Hu, J. Guo, K. C. Weerasinghe, L. Wang and W. Li, *J. Photochem. Photobiol. A: Chem.*, 2014, **274**, 57-63.
50. C. Zhao, T. Wang, D. Li, T. Lu, D. Liu, Q. Meng, Q. Zhang, F. Li, W. Li, W. Hu, L. Wang and X. Zhou, *Dyes Pigm.*, 2017, **137**, 256-264.
51. K. Gong, J. Yang, T. T. Testoff, W. Li, T. Wang, D. Liu, X. Zhou and L. Wang, *Chem. Phys.*, 2021, **549**, 111256.
52. K. C. Weerasinghe, T. Wang, J. Zhuang, H. Sun, D. Liu, W. Li, W. Hu, X. Zhou and L. Wang, *Chem. Phys. Impact*, 2022, **4**, 100062.
53. Y. Liang, M. Liu, T. Wang, J. Mao, L. Wang, D. Liu, T. Wang and W. Hu, *Adv. Mater.*, 2023, 2304820.
54. W. Feng, Z. Zengji, T. T. Testoff, T. Wang, X. Yan, W. Li, D. Liu, L. Wang and X. Zhou, *Anal. Chim. Acta*, 2021, **1153**, 338278.
55. R. Wang, K. Gong, R. Liu, D. Liu, W. Li, L. Wang and X. Zhou, *J. Porphyrins Phthalocyanines*, 2022, **26**, 469-484.
56. W. Feng, T. Wang, T. T. Testoff, C. N. Bridgmohan, C. Zhao, H. Sun, W. Hu, W. Li, D. Liu, L. Wang and X. Zhou, *Spectrochim. Acta. Part A*, 2020, **229**, 118016.
57. K. Gong, F. Xu, Z. Zhao, W. Li, D. Liu, X. Zhou and L. Wang, *Phys. Chem. Chem. Phys.*, 2023, **25**, 22002-22010.
58. K. C. Weerasinghe, T. Wang, J. Zhuang, D. Liu, W. Li, X. Zhou and L. Wang, *Comput. Mater. Sci.*, 2017, **126**, 244-251.
59. Y. Kong, H. Chen and L. Zuo, *Adv. Funct. Mater.*, 2024, 2413864.
60. H. Kaur and N. Goel, *ACS Applied Electronic Materials*, 2024, **6**, 3941-3953.
61. O. F. A. Sharif, L. M. Nhari, R. M. El-Shishtawy, M. E. M. Zayeda and A. M. Asiri, *RSC Adv.*, 2022, **12**, 19270.
62. N. Nagaraju, D. Kushavah, S. Kumar, R. Ray, D. Gambhir, S. Ghosh and S. K. Pal, *Phys. Chem. Chem. Phys.*, 2022, **24**, 3303-3311.

63. K. Morioka, K. Wakamatsu, E. Tsurumaki and S. Toyota, *Chem. Eur. J.*, 2022, **28**, e202103694.
64. Q. Wu, D. Zhao, A. M. Schneider, W. Chen and L. Yu, *J. Am. Chem. Soc.*, 2016, **138**, 7248.
65. Y. Zhang, Y. Xiao, Y. Xie, L. Zhu, D. Shi and C. Cheng, *Organic. Electronics*, 2015, **21**, 184.
66. W. Ni, M. Li, F. Liu, X. Wan, H. Feng, B. Kan, Q. Zhang, H. Zhang and Y. Chen, *Chem. Mater.*, 2015, **27**, 6077.
67. Y. Lin, J. Wang, Z.-G. Zhang, H. Bai, Y. Li, D. Zhu and X. Zhan, *Adv. Mater.*, 2015, **27**, 1170-1174.
68. J. Roncali, P. Leriche and P. Blanchard, *Adv. Mater.*, 2014, **26**, 3821.
69. H. Lu, J. Mack, Y. Yang and Z. Shen, *Chem. Soc. Rev.*, 2014, **43**, 4778.
70. J. Yang, D. Liu, T. Lu, H. Sun, W. Li, T. T. Testoff, X. Zhou and L. Wang, *Int. J. Quantum Chem.*, 2020, **120**, e26355.
71. T. Wang, M. Liu, C. Gao, Y. Song, L. Wang, D. Liu, T. Wang and W. Hu, *Dyes Pigm.*, 2022, **207**, 110734.
72. T. Wang, H. Sun, T. Lu, K. C. Weerasinghe, D. Liu, W. Hu, X. Zhou, L. Wang, W. Li and L. Liu, *J. Mol. Struct.* , 2016, **1116**, 256-263.
73. W. Feng, R. Geng, D. Liu, T. Wang, T. T. Testoff, W. Li, W. Hu, L. Wang and X. Zhou, *Org. Electronics*, 2021, **703**, 121742.
74. J. Wang and K. Rueck-Braun, *ChemPhotoChem*, 2017, **1**, 493-498.
75. H. Yao, L. Ye, H. Zhang, S. Li, S. Zhang and J. Hou, *Chem. Rev.*, 2016, **116**, 7397.
76. Z. Xie, X. Zhang, H. Wang, C. Huang, H. Sun, M. Dong, L. Ji, Z. An, T. Yu and W. Huang, *Nat. Commun.*, 2021, **12**, 3522.
77. X. Tian, L. C. Murfin, L. Wu, S. E. Lewis and T. D. James, *Chem. Sci.*, 2021, **12**, 3406-3426.
78. S. Guo, W. Dai, X. Chen, Y. Lei, J. Shi, B. Tong, Z. Cai and Y. Dong, *ACS Materials Lett.*, 2021, **3**, 379−397.
79. W. Zhao, Z. He and B. Z. Tang, *Nat. Rev. Mater.*, 2020, **5**, 869-885.
80. K. Strakova, L. Assies, A. Goujon, F. Piazzolla, H. V. Humeniuk and S. Matile, *Chem. Rev.*, 2019, **119**, 10977.
81. D. Y. Muleta, J. Song, W. Feng, R. Wu, X. Zhou, W. Li, L. Wang, D. Liu, T. Wang and W. Hu, *J. Mater. Chem. C*, 2021, **9**, 5093-5097.
82. H. Ma, Q. Peng, Z. An, W. Huang and Z. Shuai, *J. Am. Chem. Soc.*, 2019, **141**, 1010−1015.
83. J. Li, S. G. Ballmer, E. P. Gillis, S. Fujii, M. J. Schmidt, A. M. E. Palazzolo, J. W. Lehmann, G. F. Morehouse and M. D. Burke, *Science*, 2015, **347**, 1221-1226.
84. F. Xu, K. Gong, D. Liu, L. Wang, W. Li and X. Zhou, *Solar Energy*, 2022, **240**, 157-167.
85. R. Liu, D. Liu, F. Meng, W. Li, L. Wang and X. Zhou, *Dyes Pigm.*, 2021, **187**, 109135.
86. F. Xu, K. Gong, W. Fan, D. Liu, W. Li, L. Wang and X. Zhou, *ACS Appl. Energy Mater.*, 2022, **5**, 13780-13790.
87. T. T. Testoff, T. Aikawa, E. Tsung, E. Lesko and L. Wang, *Chem. Phys.*, 2022, **562**, 111641.
88. Y. Li, Z. Jia, P. Huang, C. Gao, Y. Wang, S. Xue, S. Lu and Y. M. Yang, *Energy Environ. Sci.*, 2024, DOI: 10.1039/d1034ee04378b.
89. J. Zhao and X. Zheng, *Front. Chem.*, 2022, **9**, 808957.
90. R. Bernhardt, M. Manrho, J. Zablocki, L. Rieland, A. Lützen, M. Schiek, K. Meerholz, J. Zhu, T. L. C. Jansen, J. Knoester and P. H. M. v. Loosdrecht, *J. Am. Chem. Soc.*, 2022, **144**, 19372−19381.

91. N. J. Hestand and F. C. Spano, *Chem. Rev.*, 2018, **118**, 7069.
92. J. R. Caram, S. Doria, D. r. M. Eisele, F. S. Freyria, T. S. Sinclair, P. Rebentrost, S. Lloyd and M. G. Bawendi, *Nano Lett.*, 2016, **16**, 6808−6815.
93. X. Fan, Z. Wu, L. Wang and C. Wang, *Chem. Mater.*, 2017, **29**, 639.
94. X. Fan, K. Lai, L. Wang, H. Qiu, J. Yin, P. Zhao, S. Pan, J. Xua and C. Wang, *J. Mater. Chem. A*, 2015, **3**, 12179-12187.
95. P. Besalú-Sala, M. Solà, J. M. Luis and M. Torrent-Sucarrat, *ACS Catal.*, 2021, **11**, 14467-14479.
96. S. D. Fried, S. Bagchi and S. G. Boxer, *Science*, 2014, **346**, 1510-1514.
97. I. T. Suydam, C. D. Snow, V. S. Pande and S. G. Boxer, *Science*, 2006, **313**, 200-204.
98. A. Jozeliūnaitė, S.-Y. Guo, N. Sakai and S. Matile, *Angew. Chem. Int. Ed.*, 2024, e202417333.
99. W. Diao, J. D. Farrell, B. Wang, F. Ye and Z. Wang, *J. Phys. Chem. B*, 2023, **127**, 8551-8564.
100. J. M. Bofll, W. Quapp, G. Albareda, I. d. P. R. Moreira, J. Ribas-Ariño and M. Severi, *Theor. Chem. Acct.*, 2023, **142**, 22.
101. T. M. Linker, R. Dagar, A. Feinberg, S. Sahel-Schackis, K.-i. Nomura, A. Nakano, F. Shimojo, P. Vashishta, U. Bergmann, M. F. Kling and A. M. Summers, *J. Am. Chem. Soc.*, 2024, **146**, 27563-27570.
102. V. V. Welborn, *J. Phys. Chem. B*, 2023, **127**, 9936-9942.
103. J. M. Bofill, M. Severi, W. Quapp, J. Ribas-Ariño and I. d. P. R. M. G. Albareda, *J. Chem. Phys.*, 2023, **159**, 114112.
104. X. Pan, M. Yan, Q. Liu, X. Zhou, X. Liao, C. Sun, J. Zhu, C. McAleese, P. Couture, M. K. Sharpe, R. Smith, N. Peng, J. England, S. C. E. Tsang, Y. Zhao and L. Mai, *Nat. Commun.*, 2024, **15**, 3354.
105. C. Yang, Y. Guo, H. Zhang and X. Guo, *Chem. Rev.*, 2024, doi.org/10.1021/acs.chemrev.1024c00327.
106. X. Wang, B. Zhang, B. Fowler, L. Venkataraman and T. Rovis, *J. Am. Chem. Soc.*, 2023, **145**, 11903-11906.
107. S. S. Chaturvedi, S. Vargas, P. Ajmera and A. N. Alexandrova, *J. Am. Chem. Soc.*, 2024, **146**, 16670-16680.
108. Y. Shen, Y. Mu, D. Wang, C. Liu and P. L. Diaconescu, *ACS Appl. Mater. Interfaces*, 2023, **15**, 28851–28878.
109. C. Zheng, Z. Ji, I. I. Mathews and S. G. Boxer, *Nat. Chem.*, 2023, **15**, 1715-1721.
110. H. Jabeen, M. Beer, J. Spencer, M. W. v. d. Kamp, H. A. Bunzel and A. J. Mulholland, *ACS Catal.*, 2024, **14**, 7166-7172.
111. C. Zhu, L. N. Pham, X. Yuan, H. Ouyang, M. L. Coote and X. Zhang, *J. Am. Chem. Soc.*, 2023, **145**, 21207-21212.
112. S. D. Fried and S. G. Boxer, *Annu. Rev. Biochem.*, 2017, **86**, 387-415.
113. A. Lu, Z.-P. Wu, B. Chen, D.-L. Peng, S. Yan, S. Shan, Z. Skeete, F. Chang, Y. Chen, H. Zheng, D. Zeng, L. Yang, A. Sharma, J. Luo, L. Wang, V. Petkov and C.-J. Zhong, *J. Mater. Chem. A*, 2018, **6**, 5143-5155.
114. C. Wu, Z. Xiao, L. Wang, G. Li, X. Zhang and L. Wang, *Catal. Sci. Technol.*, 2021, **11**, 1965-1973.
115. B. Miao, Z. Wu, H. Xu, M. Zhang, Y. Chen and L. Wang, *Chem. Phys. Lett.*, 2017, **688**, 92-97.

116. R. Wu and L. Wang, *J. Phys. Chem. C*, 2020, **124**, 26953-26964.
117. R. Wu, K. Sun, Y. Chen, M. Zhang and L. Wang, *Surf. Sci.*, 2021, **703**, 121742.
118. R. Wu and L. Wang, *Comput. Mater. Sci.*, 2021, **196**, 110514.
119. R. Wu, K. R. Wiegand and L. Wang, *J. Chem. Phys.*, 2021, **154**, 054705.
120. C. Wu, L. Wang, Z. Xiao, G. Li and L. Wang, *Phys. Chem. Chem. Phys.*, 2020, **22**, 724-733.
121. A. Cassidy, M. R. S. McCoustra and D. Field, *Acc. Chem. Res.*, 2023, **56**, 1909-1919.
122. M. A. Rothermund, S. J. Koehler and V. V. Welborn, *Chem. Rev.*, 2024, **124**, 13331-13369.
123. J. J. Ruiz-Pernía, K. Świderek, J. Bertran, V. Moliner and I. Tuñón, *J. Chem. Theory Comput.*, 2024, **20**, 1783-1795.
124. S. S. Chaturvedi, D. Bım, C. Z. Christov and A. N. Alexandrova, *Chem. Sci.*, 2023, **14**, 10997-11011.
125. S. Kalita, H. Bergman, K. D. Dubey and S. Shaik, *J. Am. Chem. Soc.*, 2023, **145**, 3543-3553.
126. J. K. Staffa, L. Lorenz, M. Stolarski, D. H. Murgida, O. Zebger, T. Utesch, J. Kozuch and P. Hildebrandt, *J. Phys. Chem. C*, 2017, **121**, 22274-22285.
127. S. Sarkar, J. G. Patrow, M. J. Voegtle, A. K. Pennathur and J. M. Dawlaty, *J. Phys. Chem. C*, 2019, **123**, 4926-4937.
128. B. Błasiak, A. W. Ritchie, L. J. Webb and M. Cho, *Phys. Chem. Chem. Phys.*, 2016, **18**, 18094-18111.
129. P. Deb, T. Haldar, S. M. Kashid, S. Banerjee, S. Chakrabarty and S. Bagchi, *J. Phys. Chem. B*, 2016, **120**, 4034-4046.
130. S. Sarkar, A. Maitra, S. Banerjee, V. S. Thoi and J. M. Dawlaty, *J. Phys. Chem. B*, 2020, **124**, 1311-1321.
131. I. T. Suydam and S. G. Boxer, *Biochem.*, 2003, **42**, 12050-12055.
132. D. Bhattacharyya, P. E. Videla, J. M. Palasz, I. Tangen, J. Meng, C. P. Kubiak, V. S. Batista and T. Lian, *J. Am. Chem. Soc.*, 2022, **144**, 14330-14338.
133. S. D. Fried, S. Bagchi and S. G. Boxer, *J. Am. Chem. Soc.*, 2013, **135**, 11181-11192.
134. D. Bhattacharyya, P. E. Videla, M. Cattaneo, V. S. Batista, T. Lian and C. P. Kubiak, *Chem. Sci.*, 2021, **12**, 10131-10149.
135. S. D. Fried and S. G. Boxer, *Acc. Chem. Res.*, 2015, **48**, 998-1006.
136. A. T. Fafarman, P. A. Sigala, J. P. Schwans and S. G. Boxer, *PNAS*, 2012, **109**, E299-E308.
137. M. M. Waegele, R. M. Culik and F. Gai, *J. Phys. Chem. Lett.*, 2011, **2**, 2598-2609.
138. A. Ge, P. E. Videla, G. L. Lee, B. Rudshteyn, J. Song, C. P. Kubiak, V. S. Batista and T. Lian, *J. Phys. Chem. C*, 2017, **121**, 18674-18682.
139. J. M. Kirsh, J. B. Weaver, S. G. Boxer and J. Kozuch, *J. Am. Chem. Soc.*, 2024, **146**, 6983-6991.
140. J. B. Weaver, J. Kozuch, J. M. Kirsh and S. G. Boxer, *J. Am. Chem. Soc.*, 2022, **144**, 7562-7567.
141. B. Dereka, N. Maroli, Y. M. Poronik, D. T. Gryko and A. A. Kananenka, *Chem. Sci.*, 2024, **15**, 15565-15576.
142. W. R. Lake, J. Meng, J. M. Dawlaty, T. Lian and S. Hammes-Schiffer, *J. Am. Chem. Soc.*, 2023, **145**, 22548-22554.
143. D. H. Oh, M. Sano and S. G. Boxer, *J. Am. Chem. Soc.*, 1991, **113**, 6880-6890.
144. S. G. Boxer, *J. Phys. Chem. B*, 2009, **113**, 2972-2983.
145. D. J. Hanaway and C. R. Kennedy, *J. Org. Chem.*, 2023, **88**, 106-115.

146. S. Yan, X. Ji, W. Peng and B. Wang, *J. Phys. Chem. B*, 2023, **127**, 4245-4253.
147. M. Xie, F.-Q. Bai, H.-X. Zhang and Y.-Q. Zheng, *J. Mater. Chem. C*, 2016, **4**, 10130-10145.
148. S. Vargas, S. S. Chaturvedi and A. N. Alexandrova, *J. Am. Chem. Soc.*, 2024, **146**, 28375-28383.
149. S. Dadashi, S. Parshotam, B. Mandal, B. Rehl, J. M. Gibbs and E. Borguet, *J. Phys. Chem. C*, 2024, **128**, 9683-9692.
150. H. R. Kelly, P. E. Videla, C. P. Kubiak, T. Lian and V. S. Batista, *J. Phys. Chem. C*, 2023, **127**, 6733-6743.
151. K. Gopakumar, V. Samantaray, M. K. Prusty, L. Swain and R. Ramanan, *Chem. Commun.*, 2023, **59**, 13054-13057.
152. I. Angelov, L. Zaharieva and L. Antonov, *Molecules*, 2023, **28**, 695.
153. J. L. Alvarez-Hernandez, XiaoweiZhang, KaiCui, A. P. Deziel, S. Hammes-Schiffer, N. Hazari, N. Piekut and M. Zhong, *Chem. Sci.*, 2024, **15**, 6800-6815.
154. X. Fu, W. Diao, Y. Luo, Y. Liu and Z. Wang, *J. Chem. Theory Comput.*, 2024, **20**, 8652-8664.
155. S. A. Siddiqui, S. Shaik and K. D. Dubey, *ACS Catal.*, 2024, **14**, 15108-15122.
156. S. A. Siddiqui, S. Shaik, S. Kalita and K. D. Dubey, *Chem. Sci.*, 2023, **14**, 10329-10339.
157. C. Tang, T. Stuyver, T. Lu, J. Liu, Y. Ye, T. Gao, L. Lin, J. Zheng, W. Liu, J. Shi, S. Shaik, H. Xia and W. Hong, *Nat. Commun.*, 2023, **14**, 3657.
158. M. Á. G. López, R. Ali, M.-L. Tan, N. Sakai, T. Wirth and S. Matile, *Sci. Adv.*, 2023, **9**, eadj5502.
159. D. S. Gottfried, M. A. Steffen and S. G. Boxer, *Science*, 1991, **251**, 662-665.
160. R. Reich, R. Scheerer, K.-U. Sewe and H. T. Witt, *BBA-Bioenergetics*, 1976, **449**, 285-294.
161. M. Xie, J. Wang, J. Ren, L. Hao, F.-Q. Bai, Q.-J. Pan and H.-X. Zhang, *Org. Electronics*, 2015, **26**, 164-175.
162. J. Vacek, M. Zatloukalová, V. Dorčák, M. Cifra, Z. Futera and V. Ostatná, *Microchimica Acta*, 2023, **190**, 442.
163. A. S. Klymchenko and A. P. Demchenko, *J. Am. Chem. Soc.*, 2002, **124**, 12372-12379.
164. K. Chaitanya, M. B. Heron and X.-H. Ju, *Dyes Pigments*, 2017, **141**, 501-511.
165. P. Song, Y. Li, F. Ma, T. Pullerits and M. Sun, *J. Phys. Chem. C*, 2013, **117**, 15879-15889.
166. A. D. Becke, *J. Chem. Phys.*, 1993, **98**, 5648-5652.
167. P. J. Stephens, F. J. Devlin, C. F. Chabalowski and M. J. Frisch, *J. Phys. Chem.*, 1994, **98**, 11623-11627.
168. L. L. Walkup, K. C. Weerasinghe, M. Tao, X. Zhou, M. Zhang, D. Liu and L. Wang, *J. Phys. Chem. C*, 2010, **114**, 19521-19528.
169. T. Yanai, D. P. Tew and N. C. Handy, *Chem. Phys. Lett.*, 2004, **393**, 51-57.
170. P. C. Ubaldo, N. D. Colley, K. N. Plunkett and L. Wang, *ChemRxiv*, 2022, 10.26434/chemrxiv-22022-hgmlj.
171. J. Tatum, 3.4: Potential Energy of a Dipole in an Electric Field. In Electricity and Magnetism 2024.